

Damage state analysis of seismically isolated multi-span continuous bridge

A.K.M.T.A. Khan

Institute of Earthquake Engineering Research (IEER), Chittagong University of Engineering and Technology (CUET), Chittagong-4349, Bangladesh

M.A.R. Bhuiyan

Department of Civil Engineering, Chittagong University of Engineering and Technology (CUET), Chittagong-4349, Bangladesh

ABSTRACT: This study is devoted towards conducting seismic performance and damage state analysis of a seismically isolated multi-span continuous bridge incorporating soil-structure interaction when subjected to a Far Field (FF) and a Near Fault (NF) ground motion records. Laminated Rubber Bearing (LRB), manufactured using high damping rubber is used in the seismic isolation. In seismic performance evaluation of the bridge, nonlinear dynamic analysis using a standard time integration approach has been carried out by incorporating the nonlinear mechanical behavior of High Damping Rubber Bearing (HDRB). An improved visco-elasto-plastic rheology model and the conventional bilinear model for HDRB, a bilinear force-displacement relationship for bridge pier and an equivalent linear model for footing-soil interaction are employed in the analysis. The seismic responses of the bridge system considered in the performance evaluation are deck displacement, pier displacement, foundation movement and shear strain of HDRB. The analysis results have revealed that, the modeling approaches of HDRB have significant effect on the seismic responses of isolated bridge system when subjected to NF and FF earthquakes. Finally, damage state analysis has been carried out to realize the effect of modeling approach of HDRB on seismic responses of bridge.

1 INTRODUCTION

Bridge structures possess an influential economic indicator for countrywide transportation development. It strongly supports the smooth movement of goods and lives by establishing the links between cities, urban and semi urban areas. In this regard, bridges serve as a transportation lifeline of the modern society. In view of the importance of the bridge structure, it is a contemporary key issue to minimize as much as possible the loss of the bridge functions against earthquakes to enhance continued functioning of the community life. A large number of bridge structures collapsed in recently occurred destructive earthquakes in Northridge, USA in 1994 and Kobe, Japan in 1995 have exposed inadequacy of the design of existing bridge structures, which have led engineers rethink widely on how to design bridge structures against earthquakes. These occurrences have indicated that the necessity to construct and rehabilitate bridge structures to withstand seismic forces in earthquake prone regions is more than a mere philosophy (Bhuiyan, 2009). Natural Rubber Bearing (RB), Lead Rubber Bearing (LRB), High Damping Rubber Bearing (HDRB) are worldwide used different isolation devices in bridges (Khan and Bhuiyan, 2014). Due to the capability of loads while sustaining large movements with little or no maintenance requirement, very high extensibility and compressive strength together with fatigue, abrasion and corrosion resistant characteristics, the HDRBs have been found more and more applications in recent years as seismic isolation devices in bridges (Khan, 2014). The objective of this study is to conduct seismic performance evaluation and damage state analysis (DSA) of a seismically isolated bridge system incorporating the soil-interaction when subjected to Far Field (FF) and Near Fault (NF) ground motion acceleration. Accurate DSA is effectively needed for structural risk assessment, and taking limited budget retrofitting decisions. Here, the DS based on bearing strain and pier ductility has been carefully considered.

2 MODELING OF THE BRIDGE

2.1 Physical Model

A typical interior pier of a multi-span continuous bridge, isolated by high damping rubber bearing (HDRB), is used in this study shown in Figure 1(a). The bridge consists of continuous reinforced concrete (RC) deck with pre-stressed concrete (PC) girders isolated by HDRB, installed below PC girders and supported on RC piers. The superstructure consists of 200 mm thick RC slab covered by 80 mm of asphalt layer. The mass of a single span bridge deck is 1200×10^3 kg and that of a pier is 250×10^3 kg. The substructure consists of RC pier and RC footing supported on shallow spread footing. The effective mass of the footing with surrounding soil is approximated as 180×10^3 kg. The dimensions and material properties of the bridge deck and pier with footings and isolation bearings (HDRB) are given somewhere (Khan, 2014).

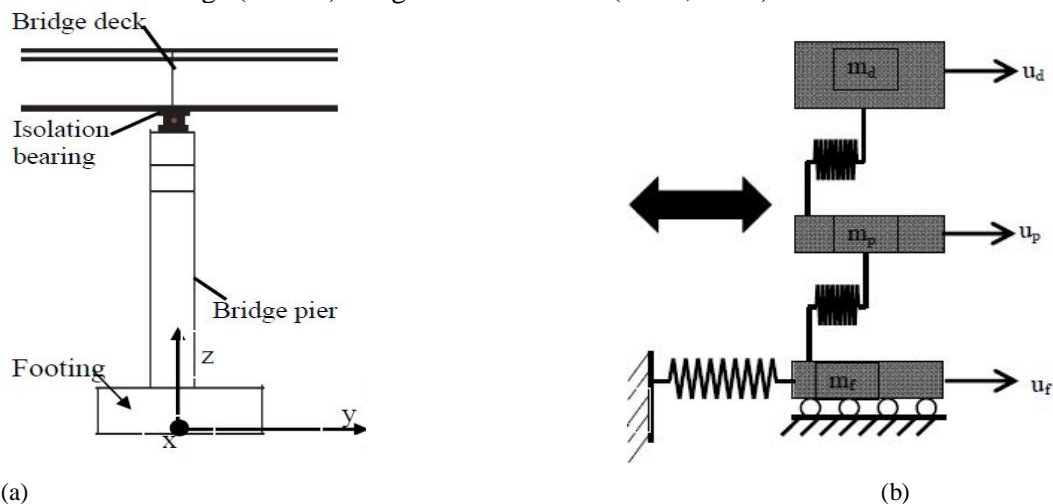


Figure 1. Modeling of the bridge pier (a) Physical Model and (b) Analytical Model

2.2 Analytical Model

The analytical model of the bridge system is shown in Figure 1(b). The bridge model is simplified into a three-degree of freedom (3-DOF) system. This simplification holds true only when the bridge superstructure is assumed to be rigid in its own plane which shows no significant structural effects on the seismic performance of the bridge system when subjected to earthquake ground motion (Alam and Bhuiyan, 2013; Khan, 2014). The mass proportional damping of the bridge pier is considered in the analysis.

3 MODELING OF HIGH DAMPING RUBBER BEARING

3.1 Original Rheology Model

The experimental investigations conducted by several authors (Bhuiyan, 2009; Khan and Bhuiyan, 2014) have revealed four different fundamental properties, which together characterize the typical overall response of laminated rubber bearings: (i) a dominating elastic ground stress response, which is characterized by large elastic strains (ii) a finite elasto-plastic response associated with relaxed equilibrium states (iii) a finite strain-rate dependent viscosity induced overstress, which is portrayed by relaxation tests, and finally (iv) a damage response within the first cycles, which induces considerable stress softening in the subsequent cycles. Considering the first three properties and motivated by the experimental observations, a visco-elastic-plastic rheology model for the HDRB and other bearing types was developed (Bhuiyan, 2009; Khan and Bhuiyan, 2014).

The model is the extended version of the Maxwell's model by adding two branches: one branch is the non-linear elastic spring element and the other one is the elasto-plastic spring-slider elements (Figure 2). The elasto-plastic and the non-linear elastic responses, which are represented in the top two branches of the model (Figure 2), constitute the rate-independent (equilibrium) hysteresis. The equilibrium hysteresis is identified from the relaxed equilibrium responses of the multi-step relaxations (MSR) of the bearings. The remaining part of the model is the rate-dependent hysteresis, which is identified from the simple relaxation (SR) and cyclic shear (CS) loading tests (Bhuiyan, 2009).

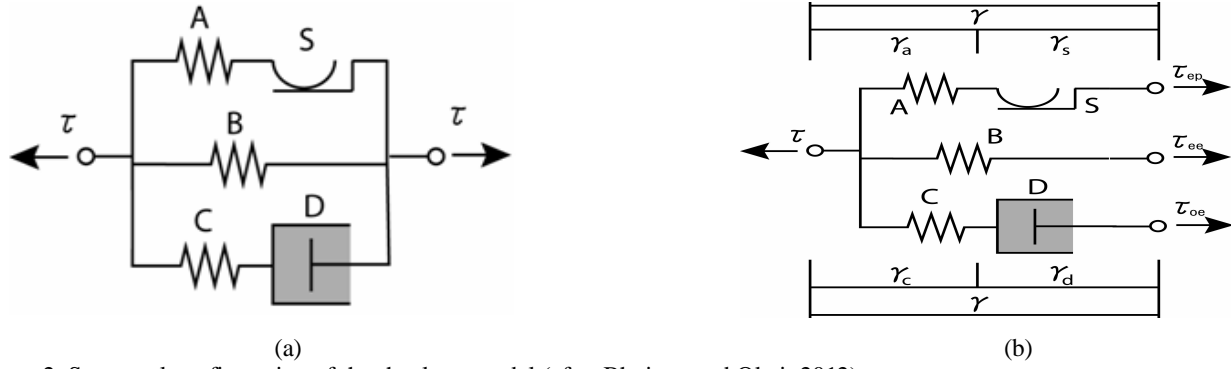


Figure 2. Structural configuration of the rheology model (after Bhuiyan and Okui, 2012)

The total stress response is phenomenologically decomposed into three components, which have been illustrated in Figure 2(b), as:

$$\tau = \tau_{ep}(\gamma_a) + \tau_{ee}(\gamma) + \tau_{oe}(\gamma_c) \quad (1a)$$

$$\tau_{ep} = C_1 \gamma_a \quad (1b)$$

$$\text{with } \begin{cases} \dot{\gamma}_s \neq 0 & \text{for } |\tau_{ep}| = \tau_{cr} \\ \dot{\gamma}_s = 0 & \text{for } |\tau_{ep}| < \tau_{cr} \end{cases}$$

$$\tau_{ee} = C_2 \gamma + C_3 |\gamma|^m \text{sgn}(\gamma) \quad (1c)$$

$$\tau_{oe} = C_4 \gamma_c \quad (1d)$$

$$\text{with } \tau_{oe} = A \left| \frac{\dot{\gamma}_d}{\dot{\gamma}_o} \right|^n \text{sgn}(\dot{\gamma}_d) \text{ and } A = \frac{1}{2} (A_1 \exp(q|\gamma|) + A_u) + \frac{1}{2} (A_1 \exp(q|\gamma|) - A_u) \tanh(\xi \tau_{oe} \gamma_d) \quad (1e)$$

where, τ_{ep} is the stress in the first branch composed of a spring (Element A) and a slider (Element S); τ_{ee} denotes the stress in the second branch with a spring (Element B); τ_{oe} represents the stress in the third branch comprising a spring (Element C) and a dashpot (Element D). The first and second branches represent the rate-independent elasto-plastic behavior, while the third branch introduces the rate-dependent viscosity behavior.

3.2 Improved Rheology Model

Considering the first three aforementioned properties, a strain-rate dependent constitutive model (i.e., Improved Rheology Model) for the HDRBs was developed and verified for sinusoidal excitations. Eq. (2a) to Eq. (2d) provides the explicit expressions for the average shear stress τ and strain γ of the bearings.

$$\tau = \tau_{ep}(\gamma_a) + \tau_{ee}(\gamma) + \tau_{oe}(\gamma_c) \quad (2a)$$

$$\tau_{ep} = C_1 \gamma_a \quad (2b)$$

$$\text{with } \begin{cases} \dot{\gamma}_s \neq 0 & \text{for } |\tau_{ep}| = \tau_{cr} \\ \dot{\gamma}_s = 0 & \text{for } |\tau_{ep}| < \tau_{cr} \end{cases} \quad \text{and } \tau_{cr} = S_1 + S_2 |\gamma_{\max}|$$

$$\tau_{ee} = C_2 \gamma + C_3 |\gamma|^m \text{sgn}(\gamma) \quad (2c)$$

$$\tau_{oe} = C_4 \gamma_c, \text{ with } \tau_{oe} = A \left| \frac{\dot{\gamma}_d}{\dot{\gamma}_o} \right|^n \text{sgn}(\dot{\gamma}_d) \quad (2d)$$

$$\text{and, } A = \frac{1}{2} (A_1 \exp(q|\gamma|) + A_u) + \frac{1}{2} (A_1 \exp(q|\gamma|) - A_u) \tanh(\xi \tau_{oe} \gamma_d) \quad (2e)$$

where, C_i ($i = 1$ to 4), S_i ($i = 1$ to 2), τ_{cr} , m , A_1 , A_u , q , n and ξ are the model parameters determined from a number of experiments and are listed somewhere (Khan, 2014) for several HDR bearing sample. Here, all the parameters express the similar meaning as like the original rheology model (Bhuiyan, 2009) except the critical shear stress τ_{cr} possess the algebraic summation of S_1 and S_2 (Khan and Bhuiyan, 2014).

3.3 Conventional Bilinear Model

It is renowned that the isolation bearing has generally nonlinear inelastic hysteretic property. Some specifications have recommended to bilinear model in order to represent the nonlinear inelastic hysteretic property of the HDRB (JRA, 1996; JRA, 2002). In this regard, three parameters are required to represent the hysteresis loop of HDRBs are initial stiffness K_1 , post yield stiffness K_2 and the characteristic yield strength Q_d of the bearings (Khan, 2014). The design equations for determining these parameters are given below:

$$K_1 = G_1 \frac{A_e}{\sum t_e} \quad (3a)$$

$$K_2 = G_2 \frac{A_e}{\sum t_e} \quad (3b)$$

$$Q_d = A_e (\gamma(G(\gamma) - G_2(\gamma))) \quad (3c)$$

$$G(\gamma) = a_0 + a_1\gamma + a_2\gamma^2 + a_3\gamma^3 + a_4\gamma^4 \quad (4a)$$

$$G_1(\gamma) = c_0 + c_1\gamma + c_2\gamma^2 + c_3\gamma^3 + c_4\gamma^4 \quad (4b)$$

$$\text{and, } G_2(\gamma) = d_0 + d_1\gamma + d_2\gamma^2 + d_3\gamma^3 + d_4\gamma^4 \quad (4c)$$

where, A_e is the cross sectional area of the bearing; $\sum t_e$ is the thickness of rubber layers; γ is the shear strain; a_i ($i=0,4$), c_i ($i=0,4$) and d_i ($i=0,4$) are the parameters which are presented somewhere (Khan, 2014). The rubber type G12 is used in manufacturing the laminated rubber bearing. The initial and post yield stiffness values along with the characteristic values used for the HDRBs are calculated using Eq. 3(a, b, and c).

3.4 Modeling of Soil Footing Interaction

It is widely accepted that the effects of the ground conditions should be considered in the seismic performance analysis of bridges, especially when the bridge utilizes the seismic isolation devices (JRA, 2002). The type of ground conditions are made in accordance with the ground characteristic value T_G (Table 1). The value of T_G can be estimated using Eq. (5).

$$T_G = 4 \sum_{i=1}^n \frac{H_i}{V_{si}}; \quad (5)$$

where, T_G is the characteristic value of soil (s), H_i is the thickness of the i^{th} soil layer (m), n is the number of soil layers and V_{si} is the average shear elastic velocity of the i^{th} soil layer which can be evaluated using the standard penetration values (N), if there is no measured value available. This value is usually measured by elastic wave propagation or PS logging (JRA, 2002). In different bridge design specifications, such as JRA (2002), it is recommended to avoid the needless complicacy in estimating the elastic shear velocity of soil layer V_{si} , rather the following equations are recommended to use for this purpose:

$$V_{si} (m/s) = 100N_i^{1/3} \quad 1 \leq N_i \leq 50 \quad \text{for cohesive soil layer} \quad (6a)$$

$$V_{si} (m/s) = 80N_i^{1/3} \quad 1 \leq N_i \leq 50 \quad \text{for sandy or cohesion-less soil layer} \quad (6b)$$

Table 1. Ground types in seismic design (JRA, 2002; Alam and Bhuiyan, 2013)

Sl. No.	Ground Type	Characteristic Value of Ground, T_G (s)
01	Type-I	$T_G < 0.2$
02	Type-II	$0.2 \leq T_G < 0.6$
03	Type-III	$0.6 \leq T_G$

The rotation of footing is usually considered only when uplift and rocking of the entire footing can occur. Considering the coordinate axes as shown in Figure 1(a) the spring constants of the ground are expressed (JRA, 1996) as:

$$\begin{Bmatrix} F_y \\ M_x \\ F_z \end{Bmatrix} = \begin{bmatrix} K_y & K_{y\theta_x} & 0 \\ K_{y\theta_x} & K_{\theta_x} & 0 \\ 0 & 0 & K_z \end{bmatrix} \begin{Bmatrix} \delta_y \\ \theta_x \\ \delta_z \end{Bmatrix} \quad (7)$$

where, F_y, F_z are the forces acting on the foundation in the y-translational and vertical (z axis) directions (tf); M_x is moment around the x-axis acting on the foundation (tf.m) δ_y, δ_z are the displacements of the foundation in the y-translational and vertical direction (z axis) (m); θ_x is rotation angle of the foundation around the x-axis (rad); K_y, K_z are the spring constants of the ground in the translational and vertical directions (tf/m); K_{θ_x} is rotational spring constant of the foundation around the x-axis (tf.m/rad); $K_{y\theta_x}$ is coupling spring constant of the foundation of the displacement in the y-direction and rotation around the x-axis (tf.m/m). Eq. (8) shows the spring constants of the ground:

$$\left. \begin{aligned} K_y &= k_{SB} A_B \\ K_z &= k_v A_B \\ K_{\theta_x} &= k_v I_B \\ K_{y\theta_x} &= 0 \end{aligned} \right\} \quad (8)$$

where, k_{SB} is the subgrade shear reaction coefficient at the bottom of the footing (tf/m³); k_v is the subgrade vertical reaction coefficient at the bottom of the foundation (tf/m³); A_B is the area of the footing at the bottom (m²); I_B is the area moment of inertia of the footing (m⁴). The vertical subgrade reaction coefficient k_v and the horizontal subgrade reaction coefficient k_{SB} are obtained from the following Eq. (9):

$$\left. \begin{aligned} k_v &= k_{vo} \left(\frac{B_v}{30} \right)^{-3/4} \\ k_{SB} &= \lambda k_v \\ B_v &= \sqrt{A_v} \end{aligned} \right\} \quad \text{with} \quad k_{vo} = \frac{1}{30} E_D \quad \text{and} \quad E_D = 2(1 + \nu_D) \frac{\gamma_s}{10g} V_{si}^2 \quad (9)$$

where, k_{vo} is the standard value of vertical subgrade reaction coefficient at the bottom of footing (kgf/cm³); k_{SB} is the horizontal subgrade reaction coefficient at the bottom of footing (kgf/cm³); A_v is the area of the footing at bottom (cm²); B_v is the equivalent surcharge width of the footing (cm); λ is the ratio of horizontal subgrade reaction coefficient to the vertical subgrade reaction coefficient; E_D is the dynamic deformation coefficient of soil (kgf/cm²); ν_D is the Poisson's ratio of soil; γ_s is the unit weight of soil (tf/m³); V_{si} is the average shear elastic velocity of the i^{th} soil layer (m/s); g is the acceleration due to gravity (9.81 m/s²).

Table 2. Foundation spring constants (K_y)

Sl. No.	Soil Type	K_y (N/m)
01	Very Hard Soil	2.6×10^{10}
02	Hard Soil	2.6×10^8
03	Medium Soil	2.6×10^6
04	Soft Soil	2.6×10^4

3.5 Equations of Motion

Equations that govern the dynamic responses of the 3-DOF system can be derived by considering the equilibrium of all forces acting on it using the d'Alembert's principle. In this case, the internal forces are the inertia forces, the damping forces, and the restoring forces, while the external forces are the earthquake induced forces. Equations of motion are given as:

$$m_d \ddot{u}_d(t) + F_{is}(u_p, \dot{u}_p, u_d, \dot{u}_d, t) = -m_d \ddot{u}_g(t) \quad (10a)$$

$$m_p \ddot{u}_p(t) + F_p(u_p, t) - F_{is}(u_p, \dot{u}_p, u_d, \dot{u}_d, t) = -m_p \ddot{u}_g(t) \quad (10b)$$

$$\text{and, } m_f \ddot{u}_f(t) - F_p(u_p, t) + F_f(u_f, \dot{u}_f, t) = -m_f \ddot{u}_g(t) \quad (10c)$$

where, $m_p, m_d, m_f, u_p, u_d, u_f$ are the masses and displacements of pier, deck and effective footing respectively. $\ddot{u}_p, \ddot{u}_d, \ddot{u}_f$ are the accelerations of pier, deck and foundation, respectively. \ddot{u}_g is the ground

acceleration. $F_p(u_p, t)$ is the internal restoring force of the pier to be evaluated by bilinear model (Alam and Bhuiyan, 2013). The nonlinear force-displacement relation (i.e. the bilinear model) is employed to take into account for the nonlinear force-displacement behavior of the bridge pier. $F_{is}(u_p, u_d, \dot{u}_p, \dot{u}_d, t)$ is the restoring force of the isolation bearings. For HDRB, it is computed using Eq. (10b) and becomes $F_{is}(u_p, u_d, \dot{u}_p, \dot{u}_d, t)$. $F_p(u_p, \dot{u}_p, t)$ is the restoring force to be evaluated by using the equivalent linear model. The equivalent linear model of the foundation is represented by a linear spring and a linear dashpot element. The rotational stiffness of the soil-foundation system is excluded from the idealized model for the purpose of simplicity. The unconditionally stable Runge Kutta 4th order method is used in the direct time integration of the equation of motion.

4 SEISMIC GROUND ACCELERATIONS

If the structure under consideration is within 10 miles (approximately 15 km) of a fault can be classified as Near Fault (NF). Ground motions outside this range are classified as Far Field (FF) motions (Khan, 2014). In the current studies, single NF and FF ground motion record was considered for the comparative analysis utilizing original rheology model, improved rheology model and conventional bilinear model when SSI incorporated. Peak Ground Acceleration (PGA) of the FF and NF earthquakes are 346.03 cm/sq.Sec and 686.83 cm/sq.Sec. EQ-1 (FF earthquake) was compared with EQ-2 (NF earthquake) as both are entitled to Level 2, Type II ground type (JRA, 2002) but EQ-1 is a FF ground motion but EQ-2 is a NF ground motion record.

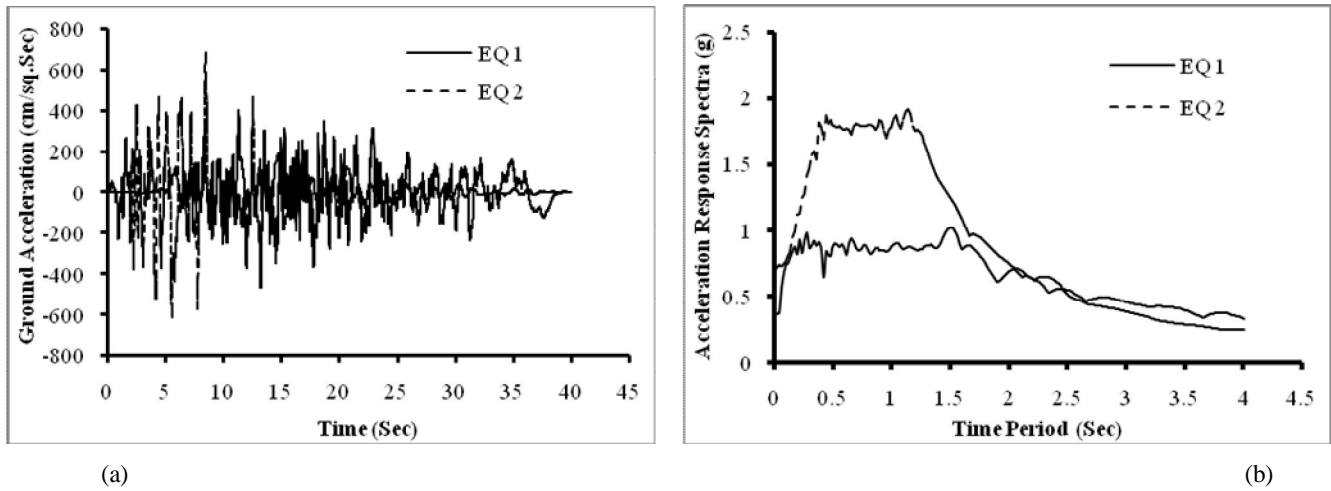


Figure 3. (a) Acceleration-time histories and (b) acceleration response spectra of FF and NF earthquake ground motion records

5 NUMERICAL OUTCOMES AND DISCUSSION

An Eigen-value analysis has been carried out to grasp the fundamental dynamic properties of the bridge. The equivalent fundamental natural period of idealized 3-DOF system is evaluated, using Eq. (11), as 1.7 sec.

$$T_e = 2\pi \sqrt{m_p \left(\frac{1}{k_f} + \frac{1}{k_p} \right) + m_f \left(\frac{1}{k_f} + \frac{1}{k_p} + \frac{1}{k_{is}} \right)} ; \quad (11)$$

where, k_f, k_p and are equivalent linear stiffness for soil-footing, pier and isolation bearing, respectively. In comparative assessment of seismic responses of the system, a few standard response parameters obtained for each earthquake are addressed in the subsequent subsections for the four types of grounds (e.g. soft, medium, hard and very hard) and is compared with that considering a fully restrained ground condition. Following expert based opinion, the numerical peak responses (deck displacement, pier displacement and bearing strain) of fully restraint soil condition for conventional bilinear model are arbitrarily assumed as 99 percent of the relevant very hard soil condition (Khan 2014). For foundation movement, the numerical peak responses of fully restraint soil condition are assumed as zero displacement.

5.1 Deck Displacement

Figure 4(a) and Figure 4(b) presents the peak responses of the deck displacement due to EQ-1 and EQ-2 as they are both entitled to Level 2 Type II earthquake but differing each other in terms of far field (EQ-1) and near fault (EQ-2) ground motion records. Figure 4(a) show that, the highest deck displacement occurs for the

soft soil condition and the lowest displacement occurs for the very hard soil condition which resulted from both improved rheology model and original rheology model. For conventional bilinear model, highest displacement occurs for medium stiff soil and lowest displacement offered by hard soil condition. On the other hand, Figure 4(b) illustrates a totally individual scenario. The highest displacement occurs for soft soil condition and lowest displacement incurred due to very hard soil condition for both improved rheology model and original rheology model. Here, the conventional bilinear model holds some different position. In this case, the highest displacement observed for medium stiff soil and lowest displacement offered by hard soil condition. The difference of the deck displacement between soft to very hard soils is quite insignificant for both the far field (EQ-1) and near fault (EQ-2) ground motion records. The direct reflection of these results can also be observed in the case of the bearing displacements. The deck displacement as obtained assuming a fully restrained condition at the base of the bridge pier is also superimposed in Figure 4(a) and Figure 4(b).

5.2 Pier Displacement

The pier displacement decreases with increase in energy dissipation but increases with increase in the bearing forces (Alam and Bhuiyan, 2013). Figure 5(a) and Figure 5(b) presents the peak responses of the pier displacement due to EQ-1 and EQ-2 as they are both entitled to Level 2 Type II earthquake but differing each other in terms of far field (EQ-1) and near fault (EQ-2) ground motion records. Figure 5(a) shows that, the highest pier displacement occurs for the soft soil condition and the lowest displacement occurs for the very hard soil condition which resulted from both improved and original rheology model. Here, conventional model holds some different position. For conventional bilinear model, highest displacement occurs for soft soil and lowest displacement offered by hard soil condition. Simultaneously, Figure 5(b) illustrates totally individual criteria. The highest pier displacement occurs for soft soil condition and lowest displacement incurred due to very hard soil condition for both original rheology model, improved rheology model and bilinear model. The difference of the pier displacement between soft to very hard soils is pretty considerable for both the far field (EQ-1) and near fault (EQ-2) ground acceleration. The pier displacements as obtained for the two earthquakes in a fully restrained ground condition are also superimposed in Figure 5(a) and Figure 5(b).

5.3 Foundation Movement

Figure 6(a) and Figure 6(b) presents the peak responses of the foundation movement due to EQ-1 and EQ-2 as they are both entitled to Level 2 Type II earthquake but differing each other in terms of far field (EQ-1) and near fault (EQ-2) ground motion records. Figure 6(a) shows that, the highest foundation movement occurs for the soft soil condition and the lowest movement occurs for the very hard soil condition which resulted from both original rheology model, improved rheology model and conventional bilinear model. On the other hand, Figure 6(b) illustrates nearly similar phenomena. The highest foundation movement occurs for soft soil condition and lowest movement incurred due to very hard soil condition for both the original rheology model, improved rheology model and conventional bilinear model. The difference of the foundation movement between soft to very hard soils is highly considerable for both the far field (EQ-1) and near fault (EQ-2) ground motion records. The foundation movements as obtained for the two earthquakes in a fully restrained ground condition are also superimposed in Figure 6(a) and Figure 6(b).

5.4 Shear Strain of High Damping Rubber Bearing

Figure 7(a) and Figure 7(b) presents the peak responses of shear strain of the isolation bearing due to EQ-1 and EQ-2 as they are both entitled to Level 2 Type II earthquake but differing each other in terms of far field (EQ-1) and near fault (EQ-2) ground motion records. Figure 7(a) confirming the highest bearing strain evolved for the very hard soil condition and the lowest strain exerts for the soft soil condition which resulted from improved rheology model and conventional bilinear model. But, original rheology model possess different trend, where the highest strain evolved for very hard soil condition but lowest strain exerts for medium stiff soil condition. On the other hand, Figure 7(b) illustrates nearly similar affinity. The highest bearing strain developed for very hard soil condition and lowest strain incurred due to soft soil condition for both original rheology model, improved rheology model and conventional bilinear model. The difference of shear strain of the isolation bearing between soft to very hard soils is not significant for both the far field (EQ-1) and near fault (EQ-2) ground motion records. The bearing strain as obtained for the two earthquakes in a fully restrained ground condition are also superimposed in Figure 7(a) and Figure 7(b) as reference values.

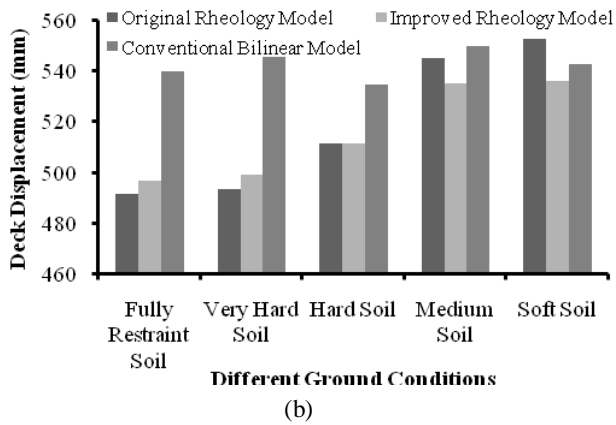
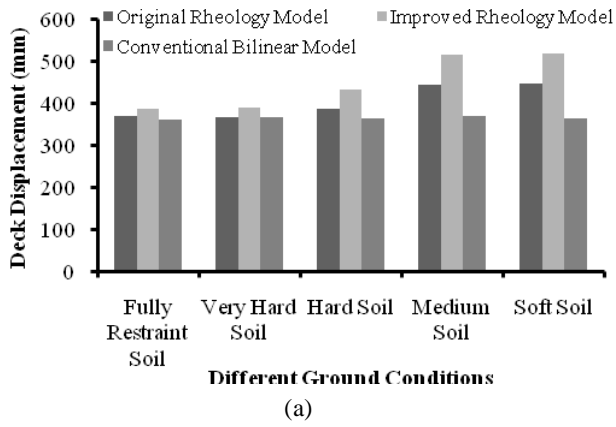


Figure 4. Peak responses of deck displacement for different ground conditions obtained from different modeling approaches when subjected to (a) far field earthquake EQ-1 and (b) near fault earthquake EQ-2

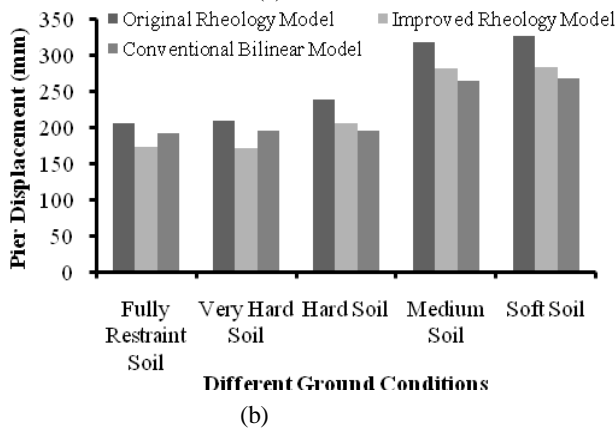
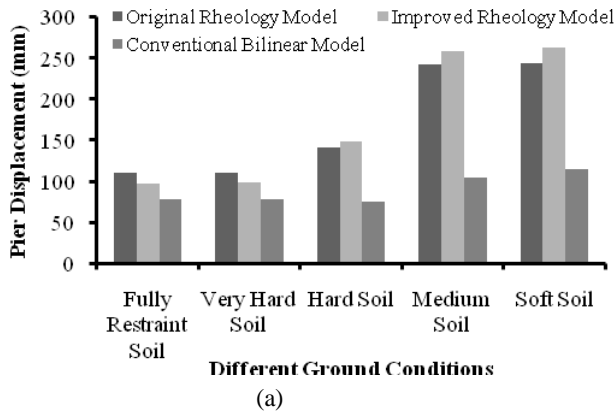
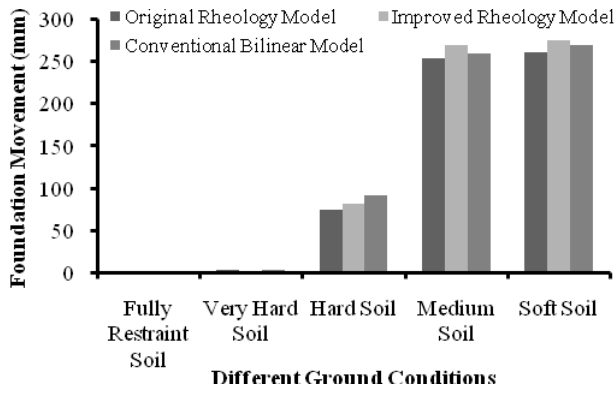
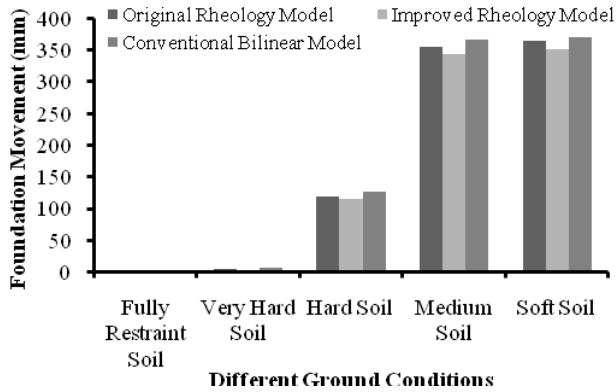


Figure 5. Peak responses of pier displacement for different ground conditions obtained from different modeling approaches when subjected to (a) far field earthquake EQ-1 and (b) near fault earthquake EQ-2

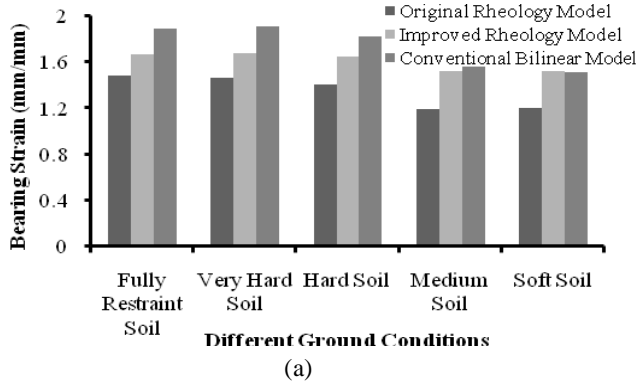


(a)

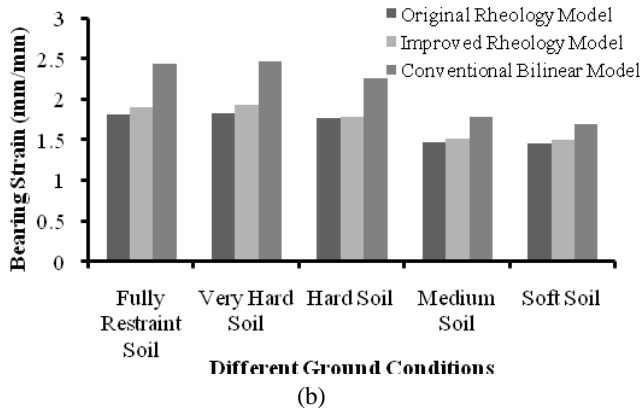


(b)

Figure 6. Peak responses of foundation movement for different ground conditions obtained from different modeling approaches when subjected to (a) far field earthquake EQ-1 and (b) near fault earthquake EQ-2



(a)



(b)

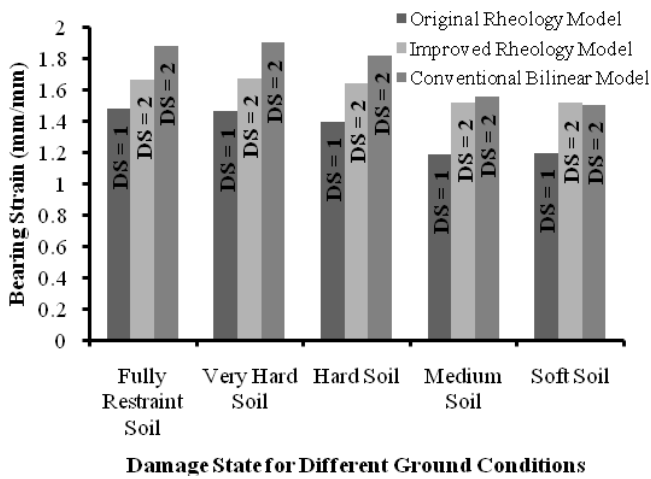
Figure 7. Peak responses of bearing strain for different ground conditions obtained from different modeling approaches when subjected to (a) far field earthquake EQ-1 and (b) near fault earthquake EQ-2

6 DAMAGE STATE ANALYSIS

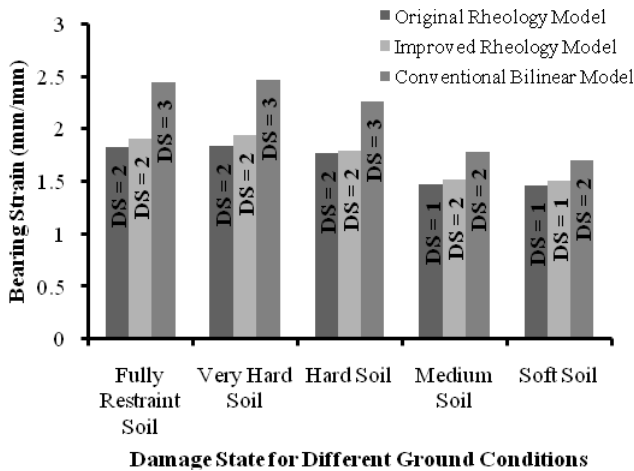
Damage state analysis might be a strong tool for risk assessment of any bridge structures. In order to identify the damage states of the bridge components, the definitions of damage states and their corresponding damage criteria available in the Table 3 (Alam and Bhuiyan, 2013; Khan, 2014). In addition to DS = 1 to DS = 4, one more damage state was considered namely DS = 0 (No Significant Physical Damage) for smooth DS analysis. Physical interpretations of different damage states also enumerates in Table 3.

Table 3. Damage/limit states of bridge components

Physical Phenomenon	Damage State	Displacement Ductility, μ_d	Shear Strain (%), γ
No significant physical damage	No Damage (DS=0)	$\mu_d \leq 1.0$	$\gamma \leq 100$
Cracking	Slight Damage (DS=1)	$\mu_d > 1.0$	$\gamma > 100$
Moderate cracking and spalling	Moderate Damage (DS=2)	$\mu_d > 1.2$	$\gamma > 150$
Degradation without collapse	Extensive Damage (DS=3)	$\mu_d > 1.76$	$\gamma > 200$
Failure leading to collapse	Total Collapse (DS=4)	$\mu_d > 4.76$	$\gamma > 250$



(a)



(b)

Figure 8. Comparison of damage states based on bearing strain for different ground condition due to (a) FF earthquake EQ-1 and (b) NF earthquake EQ-2 when considering both original rheology model, improved rheology model and conventional bilinear model

6.1 Shear Strain of Isolation Bearing

Figure 8(a) and Figure 8(b) presents the damage states of shear strain of the isolation bearing due to EQ-1 and EQ-2 as they are both entitled to Level 2 Type II earthquake but differing each other by the name of far field (EQ-1) and near fault (EQ-2) ground motion records. Figure 8(a) shows that, moderate damage (DS=2) occur

for very hard soil to soft soil condition observed from improved rheology model and conventional bilinear model. But, original model focused quite different phenomena. By this model, slight damage (DS=1) was allotted for very hard soil to soft soil condition. On the other hand, Figure 8(b) prove that, moderate damage (DS=2) occur for very hard soil condition to hard soil condition and slight damage (DS=1) occur for medium stiff soil to soft soil condition which was predicted from original rheology model. Here, improved rheology model and conventional bilinear model also deviate with the previous one. For improved rheology model, moderate damage (DS=2) was incurred for very hard to medium stiff soil condition and slight damage (DS=1) take places for soft soil condition. For conventional bilinear model, extensive damage (DS=3) was realized for very hard soil to hard soil condition and moderate damage (DS=2) performed under medium stiff to soft soil condition. The shear strain of the isolation bearing as obtained for the two earthquakes in a fully restraint ground condition are also superimposed in Figure 8(a) and Figure 8(b) as reference values.

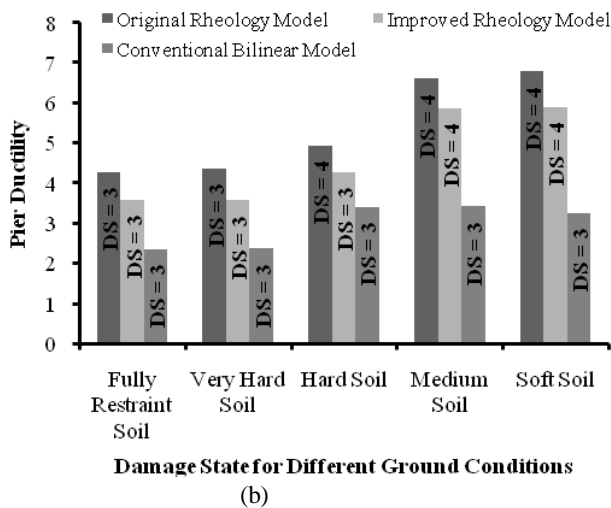
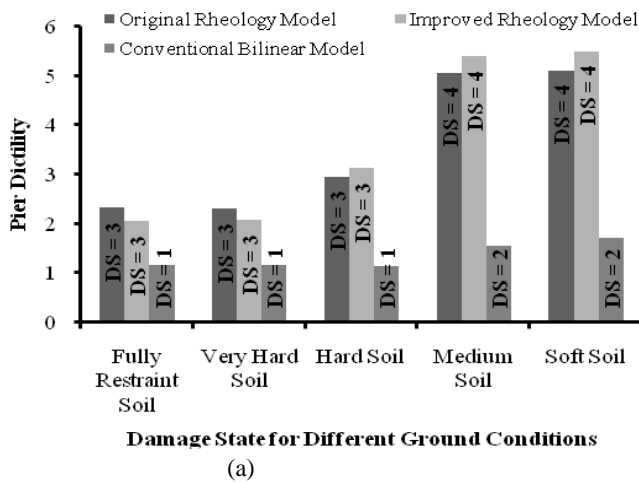


Figure 9. Comparison of damage states based on pier ductility for different ground condition due to (a) FF earthquake EQ-1 and (b) NF earthquake EQ-2 when considering both original rheology model, improved rheology model and conventional bilinear model

6.2 Displacement Ductility of Bridge Pier

Figure 9(a) and Figure 9(b) presents the damage states of ductility of the bridge pier due to EQ-1 and EQ-2 as they are both entitled to Level 2 Type II earthquake but differing each other by the name of far field (EQ-1) and near fault (EQ-2) ground motion records. Figure 9(a) shows that, extensive damage (DS=3) occur for very hard soil to hard soil condition and collapse damage (DS=4) occur for medium stiff soil to soft soil condition which was predicted from both original rheology model and improved rheology model. But, conventional bilinear model draws slight different scenario. By this model, slight damage (DS=1) was incurred for very hard soil to hard soil condition and moderate damage (DS=2) was attained for medium stiff soil to soft soil condition. On the other hand, Figure 9(b) attests that, extensive damage (DS=3) was induced for very hard soil and collapse damage (DS=4) was observed for hard soil to soft soil condition which was worked out from both original rheology model. Here, improved rheology model and conventional bilinear model also

strongly deviate with the previous one. Improved rheology model shows that, extensive damage (DS=3) was performed by very hard soil to hard soil condition and collapse damage (DS=4) was induced by medium stiff soil to soft soil condition. Conventional bilinear model shows that, extensive damage (DS=3) was observed for very hard soil to soft soil condition respectively. The ductility of the bridge pier as obtained for the two earthquakes in a fully restraint ground condition are also superimposed in Figure 9(a) and Figure 9(b) as reference values.

7 CONCLUDING REMARKS

This study presents the seismic performance assessment and corresponding DSA of a bridge pier modeled by 3-DOF system and isolated by high damping rubber bearing (HDRB). The bridge is analyzed for two earthquake ground acceleration records, namely EQ-1 and EQ-2. The nonlinearity of the bridge pier is considered by employing a bilinear force-displacement relationship, whereas a visco-elasto-plastic rheology model is employed to evaluate the mechanical behavior of HDRB under seismic excitations.

The SSI effect has been introduced by an equivalent linear model. The numerical results have revealed that the seismic responses of the bridge pier are significantly affected by the ground conditions representing the support conditions, types of input ground motion and the corresponding modeling approaches. For example, deck displacement, pier displacement and foundation movement differs with NF and FF ground motions for different ground conditions when implicated on different modeling approaches. For similar type earthquake and ground condition, the bearing strain and pier ductility evolves different DS for different modeling approaches. For bearing strain and pier ductility, the conventional bilinear model and original rheology possess more conservative modeling approach than others. In most of the cases, improved rheology model situates in between the other two models. From above study it might be conclude that the ground conditions, the ground motion records and the modeling approaches have significant effect on the seismic responses and DSA of the bridge, which should be carefully considered in the design phase of seismically isolated bridge system. In the current study, only one bridge pier with two earthquake ground records is considered; however, a more rigorous modeling of the bridge system is expected for an elaborate numerical investigation which can be dealt with in a future study.

REFERENCES

- Alam, A.K.M. T., and Bhuiyan, M. A. R., 2013. Effect of soil-structure interaction on seismic response of a seismically isolated highway bridge pier, *Journal of Civil Engineering (IEB)*, Bangladesh, 41 (2): 179-199.
- Bhuiyan, M. A. R., 2009. *Rheology modeling of laminated rubber bearings*, PhD dissertation. Graduate School of Science and Engineering, Saitama University, Japan.
- Japan Road Association (JRA) 1996. "*Specifications for highway bridges-Part V:Seismic design*", Japan.
- Japan Road Association (JRA) 2002. "*Specifications for highway bridges-Part V:Seismic design*", Japan.
- Khan, A.K.M. T. A., 2014. *An Improved Rheology Model of Laminated Rubber Bearings for Seismic Analysis of Multi-Span Highway Bridge*, M.Sc. Thesis, Dept. of Disaster and Envir. Engineering, CUET, Chittagong.
- Khan, A.K.M. T. A., and Bhuiyan, M. A. R., 2014. *An Improved Rheology Model of High Damping Rubber Bearing for Seismic Analysis*, Proceedings of the 2nd International Conference on Advances in Civil Engineering (ICACE-2014), December, CUET, Chittagong, Bangladesh, Paper No. SEE-026, pp. 438-448.